OPEN ACCESS Freely available online

PLOS ONE

Tropisms of AAV for Subretinal Delivery to the Neonatal Mouse Retina and Its Application for *In Vivo* Rescue of Developmental Photoreceptor Disorders

Satoshi Watanabe[1,2,3,4], Rikako Sanuki[1,2,3], Shinji Ueno[5], Toshiyuki Koyasu[5], Toshiaki Hasegawa[6], Takahisa Furukawa[1,2,3]*

1 Laboratory for Molecular and Developmental Biology, Institute for Protein Research, Osaka University, Suita, Osaka, Japan, 2 JST, CREST, Suita, Osaka, Japan, 3 Department of Developmental Biology, Osaka Bioscience Institute, Suita, Osaka, Japan, 4 Kyoto University Graduate School of Medicine, Sakyo-ku, Kyoto, Kyoto, Japan, 5 Department of Ophthalmology, Nagoya University Graduate School of Medicine, Showa-ku, Nagoya, Aichi, Japan, 6 Research Center for Ultra-high Voltage Electron Microscopy, Osaka University, Ibaraki, Osaka, Japan

Abstract

Background: Adeno-associated virus (AAV) is well established as a vehicle for *in vivo* gene transfer into the mammalian retina. This virus is promising not only for gene therapy of retinal diseases, but also for *in vivo* functional analysis of retinal genes. Previous reports have shown that AAV can infect various cell types in the developing mouse retina. However, AAV tropism in the developing retina has not yet been examined in detail.

Methodology/Principal Findings: We subretinally delivered seven AAV serotypes (AAV2/1, 2/2, 2/5, 2/8, 2/9, 2/10, and 2/11) of AAV-CAG-mCherry into P0 mouse retinas, and quantitatively evaluated the tropisms of each serotype by its infecting degree in retinal cells. After subretinal injection of AAV into postnatal day 0 (P0) mouse retinas, various retinal cell types were efficiently transduced with different AAVs. Photoreceptor cells were efficiently transduced with AAV2/5. Retinal cells, except for bipolar and Müller glial cells, were efficiently transduced with AAV2/9. Horizontal and/or ganglion cells were efficiently transduced with AAV2/1, AAV2/2, AAV2/8, AAV2/9 and AAV2/10. To confirm the usefulness of AAV-mediated gene transfer into the P0 mouse retina, we performed AAV-mediated rescue of the *Cone-rod homeobox* gene knockout (*Crx* KO) mouse, which exhibits an outer segment formation defect, flat electroretinogram (ERG) responses, and photoreceptor degeneration. We injected an AAV expressing *Crx* under the control of the *Crx 2kb* promoter into the neonatal *Crx* KO retina. We showed that AAV mediated-Crx expression significantly decreased the abnormalities of the *Crx* KO retina.

Conclusion/Significance: In the current study, we report suitable AAV tropisms for delivery into the developing mouse retina. Using AAV2/5 in photoreceptor cells, we demonstrated the possibility of gene replacement for the developmental disorder and subsequent degeneration of retinal photoreceptors caused by the absence of *Crx*.

Citation: Watanabe S, Sanuki R, Ueno S, Koyasu T, Hasegawa T, et al. (2013) Tropisms of AAV for Subretinal Delivery to the Neonatal Mouse Retina and Its Application for *In Vivo* Rescue of Developmental Photoreceptor Disorders. PLoS ONE 8(1): e54146. doi:10.1371/journal.pone.0054146

Editor: Alfred Lewin, University of Florida, United States of America

Received July 14, 2012; **Accepted** December 6, 2012; **Published** January 15, 2013

Funding: This work was supported by CREST and from Japan Science and Technology Agency (http://www.jst.go.jp), a grant for Molecular Brain Science, Grants-in-Aid for Scientific Research on Priority Areas, and Grant-in-Aid for Scientific Research (B) (#20390087), Young Scientists (B) (#24700360) from the Ministry of Education, Culture, Sports and Technology of Japan (http://www.jsps.go.jp/), The Takeda Science Foundation (http://www.takeda-sci.or.jp/), The Uehara Memorial Foundation (http://www.ueharazaidan.com/), Novartis Foundation (#20-10, http://novartisfound.or.jp/), The Naito Foundation (http://www.naito-f.or.jp/), Senri Life Science Foundation (#S-2144, http://www.senri-life.or.jp/), Kato Memorial Bioscience Foundation (http://www.katokinen.or.jp/), Daiichi-Sankyo Foundation of Life Science; Japanese Retinitis Pigmentosa Society Foundation, and Research Foundation for Opto-Science and Technology (http://www.jrps.org/). The funders had no role in study design, data collection and analysis, decision to publish, or preparation of the manuscript.

Competing Interests: The authors have declared that no competing interests exist.

* E-mail: takahisa.furukawa@protein.osaka-u.ac.jp

Introduction

Functional analysis of the genes expressed in the mammalian retina is essential for understanding the molecular basis for human retinal development and disease. Recent progress in techniques of comprehensive analysis of gene expression using microarray and next generation sequencing make it possible to obtain many candidate genes that are possibly associated with retinal development and disease [1,2]. Although *in vivo* analysis of candidate genes using transgenic and/or knockout mice is beneficial in revealing the *in vivo* functions of the genes, it is still expensive, time-consuming, and requires a great deal of skill. Therefore, a rapid and convenient method of *in vivo* gene transfer would be beneficial to the field. To transduce a gene into the mouse retina, *in vivo* electroporation and virus-mediated gene transfer are currently the most available methods. *In vivo* electroporation is a method in which plasmid DNA is incorporated into retinal tissue by high-voltage pulses. This method efficiently transduces DNA into rod photoreceptor cells, but much less efficiently into bipolar, amacrine, and Müller glial cells. Moreover, cone photoreceptor, horizontal, and ganglion cells are barely transduced by *in vivo* electroporation [3]. For virus-mediated transduction, retrovirus, lentivirus, adenovirus, and adeno-associated virus (AAV) have

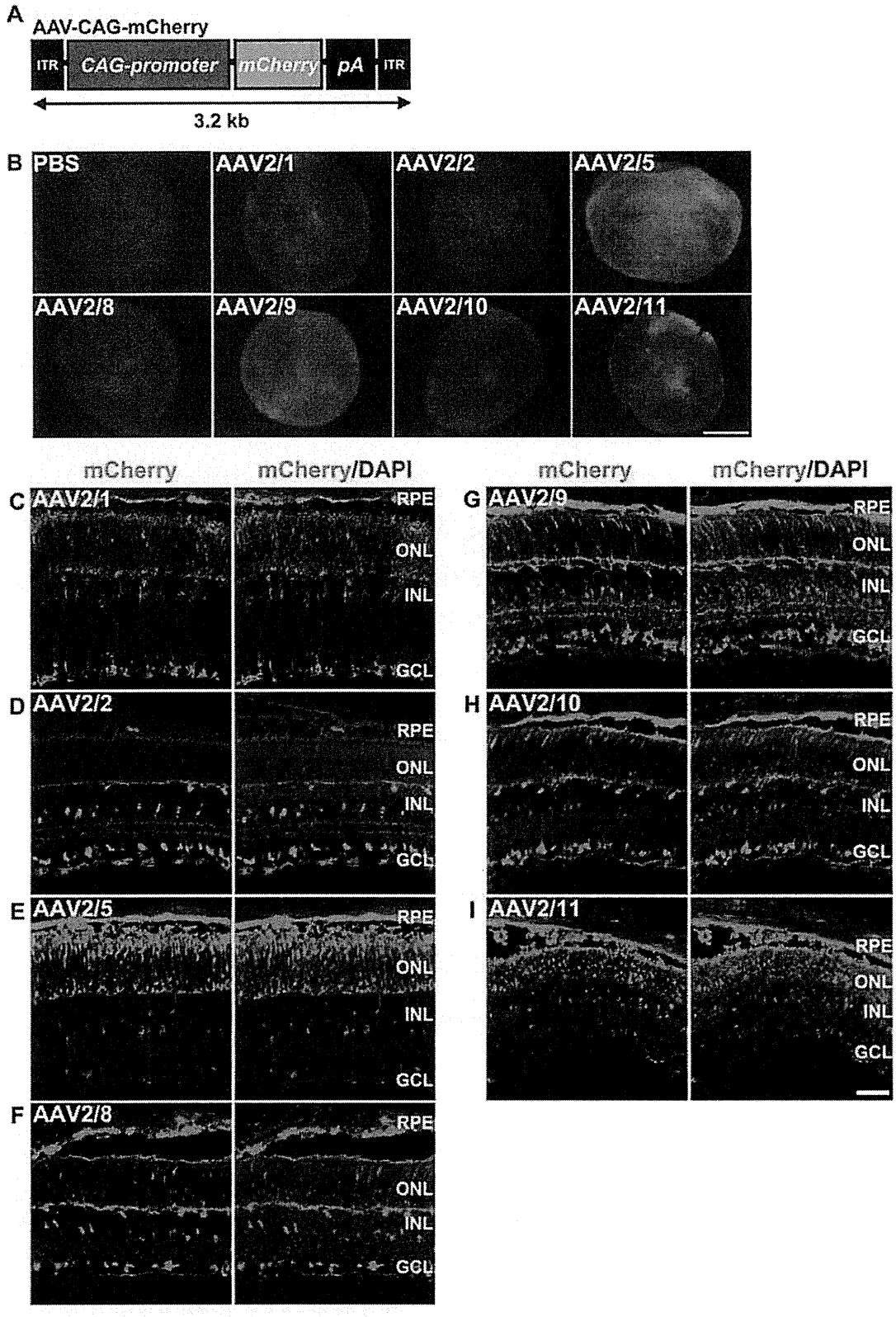

Figure 1. Tropisms of seven AAV serotypes in the P0 mouse retina. (A) Schematic diagram of the AAV-CAG-mCherry construct. This AAV drives ubiquitous expression of mCherry under the control of the *CAG* promoter. (B) Fluorescence images of the distribution of mCherry expression in

whole retinas (photoreceptor-side-up) two weeks after subretinal injection with PBS or one of each of the seven serotypes of AAV-CAG-mCherry. (C–I) Fluorescence images of mCherry expression two weeks after subretinal injection into the P0 mouse retina with AAV2/1- (C), AAV2/2- (D), AAV2/5- (E), AAV2/8- (F), AAV2/9 (G), AAV2/10- (H), and AAV2/11- (I), CAG-mCherry. Scale bar represents 1 mm (B) and 50 μm (C–I). ITR: inverted terminal repeat, RPE: retinal pigment epithelium, ONL: outer nuclear layer, INL: inner nuclear layer, GCL: ganglion cell layer.
doi:10.1371/journal.pone.0054146.g001

been developed as vehicles for retinal gene transfer. In particular, AAV has many advantages for retinal gene transfer, including high transduction efficiency in non-dividing cells, long-term transgene expression, and low-toxicity. AAV is a non-pathogenic parvovirus, which consists of single-stranded DNA covered with capsid proteins. Each AAV serotype is different in the capsid structure, which leads to different tropisms and transduction efficiencies. Twelve serotypes have currently been used as a vehicle for *in vivo* gene transfer (AAV2/1-AAV2/12). AAV tropisms for gene transduction into several murine organs and tissues, including the retina, are different according to developmental stage (neonatal or adult) [4,5]. The previous studies on AAV serotype tropism in subretinal injections into the adult mouse retina revealed that retinal pigment epithelium (RPE) cells are efficiently transduced with AAV2/1, and RPE and photoreceptor cells are efficiently transduced with AAV2/2, AAV2/5 [6,7], and AAV2/8 [7]. However, detailed AAV tropisms for transduction into the developing mouse retina have not been reported.

In the current study, we examined the tropism of seven AAV serotypes (AAV2/1, AAV2/2, AAV2/5, AAV2/8, AAV2/9, AAV2/10, and AAV2/11) by subretinal injection into the P0 mouse retina. We revealed that AAV can transduce encoded genes into various retinal cell types in the developing mouse retina. In addition, to validate the usefulness of AAV-mediated gene transfer into the developing mouse retina, we performed AAV-mediated rescue of *Crx* KO mice. CRX is a transcription factor that is predominantly expressed in photoreceptor cells and is essential for photoreceptor maturation [8,9,10]. We previously reported that *Crx* KO mice exhibit a total lack of outer segment formation, an absence of both scotopic and photopic electroretinograms (ERG), and progressive photoreceptor degeneration [10]. Our AAV-mediated rescue experiment led to a partial restoration of morphological and functional characteristics in the *Crx* KO retina. In humans, the mutations of *Crx* are associated with three forms of retinal degeneration, including cone and rod dystrophy (CORD) [11,12,13], retinitis pigmentosa (RP) [13], and Leber congenital amaurosis (LCA) [13,14], all of which can lead to vision loss. Thus, our results also provide a clue to the suitability of gene therapy for development disorders and degeneration of the retina in humans.

Results

Tropisms of Seven AAV Serotypes to the Neonatal Mouse Retina

In order to examine AAV tropisms for subretinal delivery into the P0 mouse retina, we generated AAV2/1-, AAV2/2-, AAV2/5-, AAV2/8-, AAV2/9-, AAV2/10-, and AAV2/11-vectors expressing *mCherry* driven by the ubiquitous promoter, *CAG* promoter (AAV-CAG-mCherry) (Fig. 1A). We selected six serotypes (AAV2/1, 2/2, 2/5, 2/8, 2/9, 2/10), because they are known to be infectious to the mammalian central nervous system (Gene therapy program at university of Pennsylvania (http://www.med.upenn.edu/gtp/)), and have previously been examined for tropisms for subretinal or intravitreal transduction into the adult mouse retina [6,7,15]. Since the AAV2/11 serotype was recently discovered [16], we also tested this serotype in addition to the other six. Each of the seven tested serotypes of AAV was subretinally injected into the P0 mouse retina. We harvested the injected retinas at 14 days after injection, P14, when all retinal cells had finished generating (Fig. 1B–I). We observed that mCherry expression was evenly distributed in the retinas injected with each of the seven serotypes of AAV-CAG-mCherry (Fig. 1B). AAV2/5- and AAV2/9-injected retinas showed intense mCherry signals throughout, and AAV2/2-, AAV2/8-, and AAV2/10-injected retinas showed substantial mCherry signals (Fig. 1B). Photoreceptor cells were efficiently transduced with AAV2/1, AAV2/5, AAV2/9, and AAV2/11 (Fig. 1C, E, G, I). In particular, the AAV2/5-injected retina showed mCherry expression predominantly in photoreceptor cells (Fig. 1E). The AAV2/9-injected retina showed mCherry expression throughout the retina (Fig. 1G). Horizontal cells were efficiently transduced with AAV2/1, AAV2/2, AAV2/8, AAV2/9, and AAV2/10 (Fig. 1C, D, F–H). Müller glial cells were efficiently transduced with AAV2/1 (Fig. 1C). In addition, the RPE was well transduced with all serotypes (Fig. 1C–I).

Infection Efficiencies of Seven AAV Serotypes

To quantitatively assess the tropism of seven AAV serotypes in the mouse retina, we measured the infection efficiencies for each retinal cell type. Infection efficiency is calculated by the percentage of cells expressing mCherry out of retinal cell-specific marker-positive cells (Fig. 2A). Photoreceptor and horizontal cells were efficiently transduced with AAV2/1 (Fig. 2B, Rod: 65.5±3.9% in the middle area, Cone: 80.8±4.5% and horizontal: 55.6±9.2%). The AAV2/1-injected retinas also exhibited the highest efficiency for Müller glial cells among seven serotypes (Fig. 2B, 47.9±5.8%). AAV2/2 and AAV2/8 showed similar transduction patterns with each other, and horizontal and ganglion cells were transduced mainly with these serotypes (Fig. 2C, E, horizontal cells: 78.2±3.2% and 76.6±12.2% respectively; ganglion cells: 46.9±9.4% and 40.7±0.1% respectively). AAV2/5 displayed the highest infection efficiency for rod and cone photoreceptor cells (Fig. 2D, rod; 84.5±10.3% in middle area and cone; 92.2±4.4%). Retinal cells except for bipolar and Müller glial cells were efficiently infected with AAV2/9, and infection efficiencies of AAV2/9 for horizontal and ganglion cells were the highest among seven serotypes (Fig. 2F, horizontal; 92.7±0.6% and ganglion; 82.0±0.1%). AAV2/9 showed the highest efficiency in amacrine cells (Fig. 2F, 34.8±3.2%). AAV 2/10 efficiently targeted horizontal and ganglion cells (Fig. 2G, horizontal cells: 81.0±9.9% and ganglion cells: 72.1±0.1%). AAV2/11 showed efficient infection in photoreceptor cells (Fig. 2H, rod: 70.0±8.6% in middle area and cone: 56.3±8.2%). Bipolar cells exhibited very low efficiency or no infection detected among all analyzed serotypes (Fig. 2B–H).

AAV-mediated Rescue Experiment for the *Crx* KO Retina

To validate the usefulness of AAV-mediated gene transfer into the developing mouse retina, we performed an AAV-mediated rescue experiment for the *Crx* KO mice. CRX is a transcription factor which plays a crucial role in photoreceptor maturation through photoreceptor gene transactivation [1,8,9,10]. We generated an AAV2/5 vector expressing Flag-tagged *Crx* cDNA under the control of the *Crx 2kb* promoter to drive specific expression in photoreceptor cells (AAV2/5-Crx2kb-Flag-Crx = AAV-Crx) [17,18] (Fig. 3A). We injected AAV-Crx subretinally into *Crx*

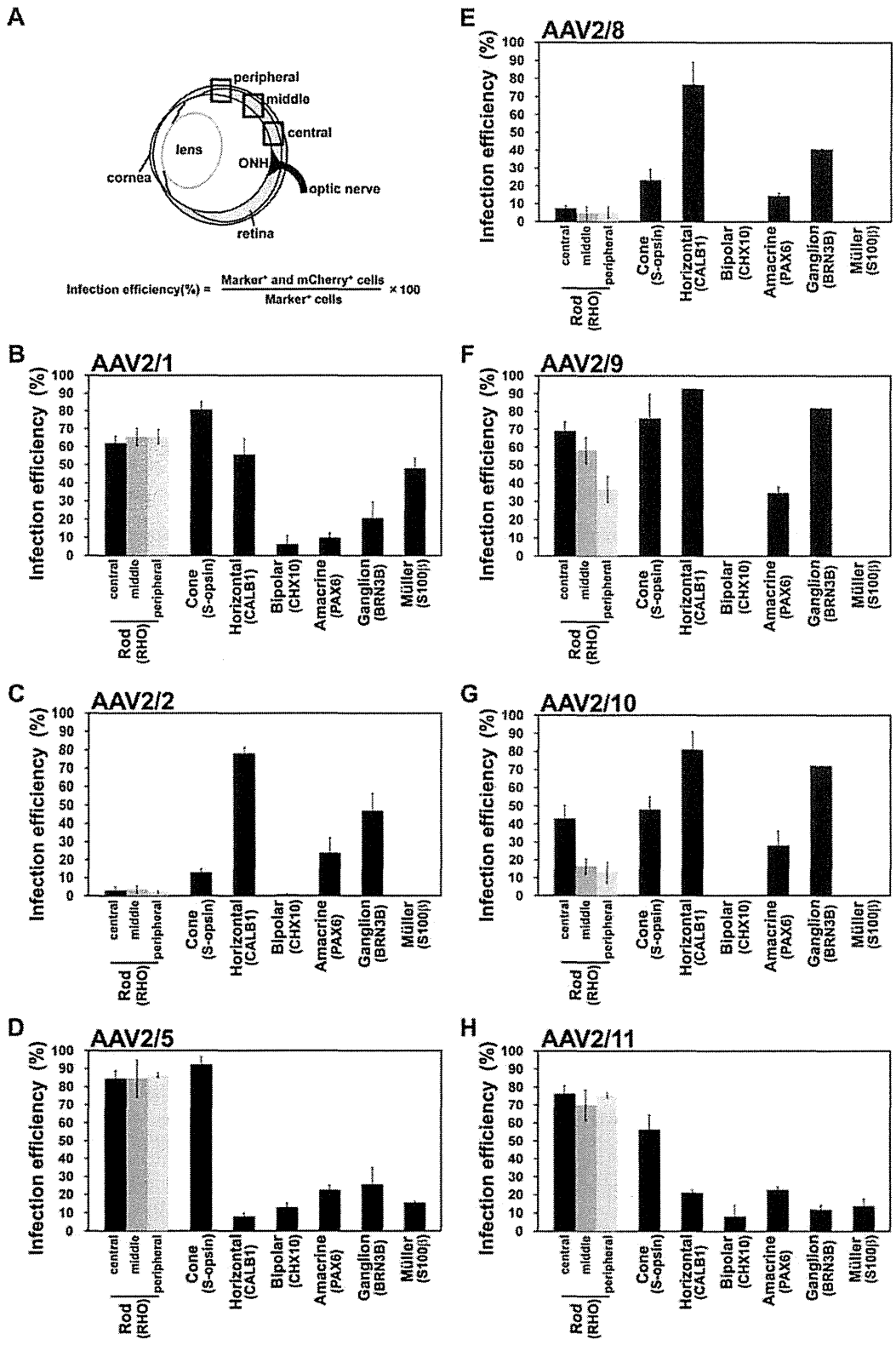

Figure 2. Infection efficiencies of seven AAV serotypes in each retinal cell type. (A) Schematic diagram of quantification method of infection efficiency. Two weeks after subretinal injection, the retinas were immunostained with antibodies of retinal cell type-specific makers (Rod:

RHODOPSIN (RHO), Cone: S-OPSIN, Horizontal: CALB1, Bipolar: CHX10, Amacrine: PAX6, Ganglion: BRN3B, Müller: S100β). According to retinal cell types, the numbers of marker-positive and marker/mCherry double-positive cells were counted for calculation of infection efficiency (n = 3 from three different mice). Cells were counted in the central area of the retina for calculating the infection efficiencies of cone photoreceptor, bipolar, and Müller glial cells, and in the central, middle and peripheral areas of the retina for calculating the infection efficiencies of rod photoreceptor and amacrine cells. Infection efficiency was calculated using the formula indicated in Figure 2A. (B–H) Infection efficiencies of AAV2/1- (B), AAV2/2- (C), AAV2/5- (D), AAV2/8- (E), AAV2/9- (F), AAV2/10- (G), and AAV2/11- (H), CAG-mCherry. Error bar represents the SD from the means of three retinas. ONH: optic nerve head.

doi:10.1371/journal.pone.0054146.g002

KO retinas at P0. To confirm the *Flag-Crx* expression in the retina, we performed an RT-qPCR analysis using RNA from the whole retina at three weeks after injection. We observed significant expression of *Flag-Crx* mRNA in the *Crx* KO retinas treated with AAV-Crx (Fig. 3B). We further analyzed FLAG-CRX expression in control and AAV-Crx treated retinas by western blotting using an anti-FLAG antibody. We detected a 38 kDa FLAG-CRX band in the AAV-treated *Crx* KO retinal lysates (Fig. 3C). To determine whether FLAG-CRX is expressed in photoreceptor cells, we performed an immunostaining of the control *Crx* KO and AAV-Crx-injected *Crx* KO retinas with the anti-FLAG antibody. FLAG signals were predominantly detected in photoreceptor cells in AAV-Crx-treated *Crx* KO retinas (Fig. 3D). Non-specific signals were also detected in the RPE and blood vessels in the INL in both control and AAV-Crx-treated *Crx* KO retinas. This is very likely due to autofluorescence from the RPE and to the reaction of the anti-mouse secondary antibody to endogenous mouse antibodies in the blood vessels (Fig. 3D). AAV-Crx-mediated FLAG-CRX expression was widely distributed throughout the AAV-Crx-treated *Crx* KO retinas (Fig. 3E, F).

The expression profiling of the *Crx* KO retina using microarray identified a number of photoreceptor genes down-regulated in the *Crx* KO retina involved in phototransduction, ciliary function, transcriptional regulation of photoreceptor genes, and synaptic development [10,19]. In humans, mutations of some of these gene homologues cause retinal diseases, including retinal degeneration, color blindness and night blindness (RetNet: https://sph.uth.tmc.edu/retnet/). Down-regulation of these genes is likely to underlie the phenotypes of the *Crx* KO retina. Thus, we performed an expression analysis of photoreceptor genes, which are down-regulated in the *Crx* KO retina and related to human retinal diseases, in AAV-Crx-treated *Crx* KO retinas. We performed RT-qPCR analyses on the following eleven genes: *Rhodopsin* (phototransduction, RP and Congenital stationary night blindness (CSNB)), *Gnat1* (phototransduction, CSNB), *S-opsin*, *M-opsin* (phototransduction, color blindness), *Pde6g* (phototransduction, RP), *Slc24a1* (phototransduction, CSNB), *Rdh12* (visual cycle, LCA and RP), *Rpgrip1* (ciliary function, LCA and CORD), *Nrl* (transcription regulation, RP), *Cabp4* (synaptic function, CSNB, LCA), and *Fscn2* (Cytoskeleton regulation, RP and macular dystrophy). In AAV-*Crx*-treated *Crx* KO retinas, we observed substantial up-regulation of *S-opsin*, *M-opsin*, and *Fscn2* (Fig. 3I, J, Q) and modest up-regulation of *Rhodopsin*, *Gnat1*, *Pde6g*, *Slc24a1*, *Rdh12*, *Rpgrip1*, *Nrl*, and *Cabp4* (Fig. 3G, H, K–P).

Immunohistochemistry of *Crx* KO Retinas Treated with AAV-Crx

We further analyzed the expression of RHODOPSIN, GNAT1, S-OPSIN, and M-OPSIN in AAV-Crx-treated *Crx* KO retinas by immunostaining. The RHODOPSIN protein level was slightly increased in AAV-Crx-injected *Crx* KO retinas (Fig. 4A–D), while GNAT1 signals were markedly increased (Fig. 4E–H). Similarly, S-OPSIN and M-OPSIN signals were markedly increased (Fig. 4I–P). Consistent with the results of the RT-qPCR analysis shown in Figure 3G–Q, the levels of these molecules also increased in AAV-Crx-treated *Crx* KO retinas. In addition, GNAT1, S-OPSIN, and M-OPSIN signals appeared to be localized in outer segments in AAV-Crx-injected *Crx* KO retinas (Fig. 4E–P). RHODOPSIN and GNAT1 are localized in the rod outer segment and S-OPSIN and M-OPSIN are localized in the cone outer segment. The *Crx* KO retina lacks outer segment formation [10,20]. This immunohistochemical data suggests that the defect of outer segment formation in the *Crx* KO retina was partially restored by the subretinal injection of AAV-Crx into *Crx* KO retinas.

We further examined the morphology of the outer segment in the control *Crx* KO and AAV-Crx-injected *Crx* KO retinas in detail by transmission electron microscopy at fifteen weeks after AAV treatment (Fig. 4Q–S). We observed no photoreceptor cells in control retinas because of severe photoreceptor degeneration in the *Crx* KO retina (Fig. 4Q). In contrast, outer segments containing disk lamina were observed in AAV-Crx-injected *Crx* KO retinas (Fig. 4R, S). These data showed that the subretinal delivery of AAV-Crx into P0 *Crx* KO retinas partially restored outer segment formation in the *Crx* KO mice.

The Improvement of Retinal Function in the *Crx* KO Retina Treated with AAV-Crx

To evaluate the effect of the AAV-Crx injection on retinal function, we performed electroretinogram (ERG) recordings. *Crx* KO mice exhibit flat scotopic and photopic ERG responses at P30, resulting from the defect of formation of outer segments and considerable loss of phototransduction molecules in the *Crx* KO mice [10]. At 6 and 15 weeks after AAV treatment, we measured ERG responses from three control and three AAV-Crx-treated eyes. The mice used for ERG recordings were independently prepared between the two time points. We first tried to record scotopic ERG responses from the AAV-treated mouse eyes in a conventional way [21,22], but no positive response was detected. Therefore, we then measured photopic ERG responses with one hundred stroboscopic flashes of 1.0 log cd-s/m^2. The ERG responses obtained under these conditions majorly reflect cone photoreceptor functions. Consistent with our previous observation [10], all of the control eyes exhibited completely flat responses at both 6 and 15 weeks after AAV treatment (Fig. 5A top, Table 1). In contrast, two of three AAV-Crx-treated eyes showed significant photopic a- and b-waves at both 6 and 15 weeks after AAV treatment (Fig. 5A bottom, Table 1). One of the AAV-Crx-treated *Crx* KO mice did not show a detectable ERG photopic response. Although this mouse eye widely expressed FLAG-CRX, the eye was much smaller than the other two mouse eyes and was severely damaged histologically (data not shown), probably due to subretinal injection damage, resulting in physiological dysfunction. This result shows that the subretinal injection of AAV-Crx into *Crx* KO retinas partially restored the physiological function of *Crx* KO photoreceptor cells.

Progressive photoreceptor degeneration is also observed in the *Crx* KO mice [10]. We examined photoreceptor degeneration in the retinas fifteen weeks after AAV treatment by immunostaining using an anti-FLAG antibody (Fig. 5B). Although there was substantial photoreceptor cell death in both control and AAV-Crx-

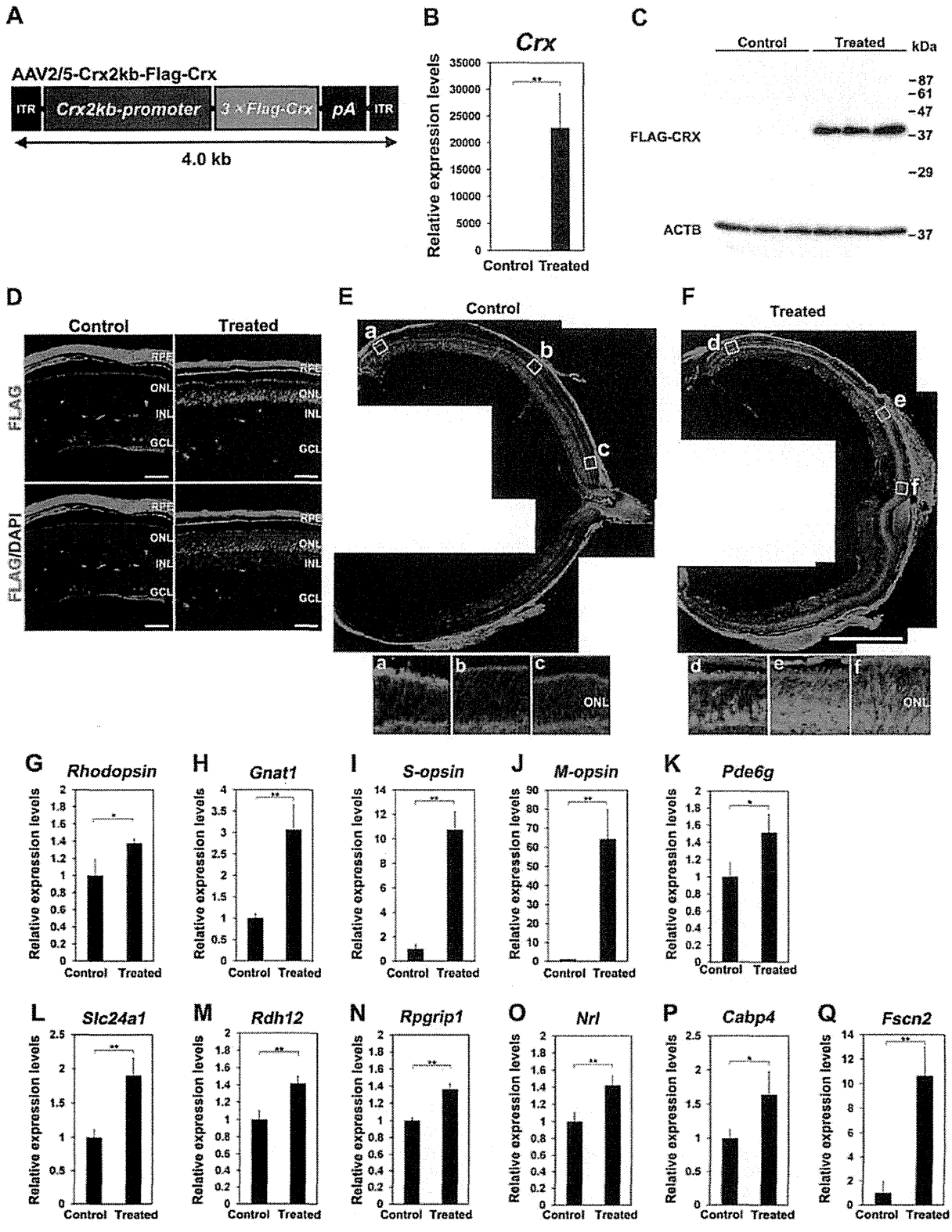

Figure 3. Gene expression analysis of the *Crx* KO retina treated with AAV-Crx. (A) Schematic diagram of the AAV2/5-Crx2kb-Flag-Crx construct. (B) Expression analysis of *Crx* by RT-qPCR using RNA isolated from control and AAV-treated *Crx* KO retinas (Control *Crx* KO retinas: n = 3 from three different mice and AAV-treated *Crx* KO retinas: n = 4 from four different mice). (C) Western blot analysis of FLAG-CRX using control and

AAV-treated *Crx* KO retinas from three different mice respectively. An anti-FLAG antibody was used to detect FLAG-CRX. ACTB (β-actin) was used as a loading control. (D–F) Immunostaining of the *Crx* KO retinas treated with AAV-Crx or PBS using an anti-FLAG antibody. The distribution of FLAG-CRX expression in control and AAV-Crx treated *Crx* KO retinas (E, F). Enlarged images in white boxes (a-c and d-f) in Figure 3E and F, respectively. Scale bar represents 50 μm (D) and 1 mm (E, F). (G–Q) Expression analyses of eleven genes related to human retinal diseases three weeks after treatment (Control *Crx* KO retinas: n = 3 from three different mice and AAV-treated *Crx* KO retinas: n = 4 from four different mice). *Rhodopsin* (G), *Gnat1* (H), *S-opsin* (I), *M-opsin* (J), *Pde6g* (K), *Slc24a1* (L), *Rdh12* (M), *Rpgrip1* (N), *Nrl* (O), *Cabp4* (P), and *Fscn2* (Q). Control retinas were injected with PBS (Vehicle). *Rpl4* was used for normalization. Primers for qPCR were listed in Table S1. Error bar represents the SD from the means of three control retinas and four treated retinas. $^{**}p<0.01$, $^{*}p<0.05$. ITR: inverted terminal repeat, RPE: retinal pigment epithelium, ONL: outer nuclear layer, INL: inner nuclear layer, GCL: ganglion cell layer.
doi:10.1371/journal.pone.0054146.g003

treated *Crx* KO retinas, AAV-Crx-treated *Crx* KO retinas had a thicker outer nuclear layer than that of control retinas (Fig. 5B top panels). Remarkably, most of the surviving photoreceptor cells in AAV-Crx-treated *Crx* KO retinas expressed FLAG-CRX (Fig. 5B bottom panels). This observation suggests that photoreceptor cells without FLAG-CRX expression died and that AAV-Crx inhibited photoreceptor cell death in the *Crx* KO retinas. To confirm this result, we performed immunostaining with an anti-active-caspase-3 antibody, an apoptosis marker, three weeks after AAV treatment (Fig. 5C, D). We observed a significant reduction of apoptotic cell numbers in AAV-Crx-treated *Crx* KO retinas (Fig. 5C, D). These results show that subretinal injection of AAV-Crx prevented photoreceptor cell death to some extent in the *Crx* KO retina.

Discussion

The main goal of this study is to establish a method for AAV-mediated retinal gene transfer into developing retinas for *in vivo* analysis of retinal genes and to apply the method to the rescue of retinal degeneration. Through the transduction of AAV-CAG-mCherry into the developing mouse retina, we showed that various retinal cell types were transduced differently with each of seven serotypes of AAV. We quantitatively analyzed infection efficiencies of these AAV serotypes. In addition, we demonstrated the usefulness of AAV transduction into the developing mouse retina for the rescue of the retinal degeneration of *Crx* KO mice. These results will be useful to researchers who perform *in vivo* analysis of retinal genes using AAV.

We subretinally injected seven serotypes of AAV into the P0 mouse retina. We chose P0, because the retina at this stage is still developing and amenable to surgical treatment by subretinal injection. Serotypes AAV2/5 and AAV2/9 exhibited remarkable and efficient infection. Photoreceptor cells were selectively and efficiently transduced with AAV2/5. Retinal cells, except for Müller glial cells and bipolar cells, were efficiently transduced with AAV2/9. We observed efficient transduction into horizontal and/or ganglion cells with AAV2/1, AAV2/2, AAV2/8, AAV2/9 and AAV2/10. These data suggests that *in vivo* gene transfer by subretinal injection of AAV into the mouse retina enables us to analyze gene function in retinal cell types that are difficult or impossible to transduce by *in vivo* electroporation (cone photoreceptor, horizontal, and ganglion cells) [3]. To perform an analysis specifically in a certain cell type in the retina, a cell type-specific promoter of relatively short length for each cell type will need to be developed in the future.

In the current study, the infection efficiencies of AAV into bipolar and Müller glial cells were low in all tested serotypes, although AAV2/1 efficiently targeted Müller glial cells. These two retinal cells undergo differentiation at the latest stages during development [21]. In contrast, retinal cells, which are generated at embryonic stages or at early postnatal stages (photoreceptor, horizontal, amacrine and ganglion cells), were transduced with all analyzed serotypes. These results suggest that the AAV serotypes tested in this study are more infectious to differentiated retinal cells than to retinal progenitor or differentiating cells. Since more than 100 AAV serotypes have been isolated [22], AAV serotypes which are capable of efficiently infecting bipolar and Müller glial cells may be found in the future. Our observations on AAV tropism in the developing retina in the current study may expand the application of AAV for *in vivo* transduction to retinal cell types, such as cone photoreceptors, horizontal cells, and ganglion cells, which are barely transduced by *in vivo* electroporation.The AAV tropisms shown in the current study were different from those for the adult mouse retina in previous reports. In subretinal transduction into the adult retina AAV2/1 mainly targets RPE cells, and AAV2/2, 2/5, and 2/8 mainly target both RPE and photoreceptor cells [6,7]. However, based on our results using P0 mice, each AAV serotype targeted several retinal cell types. This observation is consistent with the results reported by Surace *et al.* [5], in which they showed the difference of tropisms for transduction into fetal, neonatal and adult retinas using AAV2/1-, 2/2-, and 2/5-CMV-EGFP. There are two possible explanations for the shift of AAV tropism between the developing retina and the mature retina. The first is that the expression or abundance of AAV receptors in host retinal cells may change during retinal development. The second is that injected virus particles may more easily diffuse across the retina due to the smaller size of the P0 retina and dynamic cell migration during retinal development. The differences of AAV tropisms between neonatal and adult mice are also observed in the aorta, liver and kidney [4]. This suggests that the time point of transduction of an AAV vector during development is important to appropriately perform gene transfer to a cell type of interest.

We attached the *Crx 2kb* promoter to the AAV vector for the rescue experiment on the *Crx* KO retina. We previously reported that this promoter directs specific gene expression in developing and mature rod and cone photoreceptor cells [17,18]. Expression analysis by RT-qPCR and immunohistochemistry showed improved expression of both rod-specific genes (*Rhodopsin* and *Gnat1*) and cone-specific genes (*S-opsin* and *M-opsin*) in AAV-Crx-treated *Crx* KO retinas (Fig. 3G–Q and 4A–P). This indicates that the *Crx 2kb* promoter successfully drove the *Crx* expression in both rod and cone photoreceptor cells. Thus the *Crx 2kb* promoter can be used with AAV to drive expression specifically in photoreceptor cells.

AAV-Crx modestly but significantly improved the photopic ERG responses, but we were not able to detect scotopic ERG responses in AAV-treated eyes. In order to detect relatively weak ERG responses in AAV-Crx-treated *Crx* KO eyes, we stimulated the mouse eyes with one hundred stroboscopic flashes (1.0 log cd-s/m^2). However, under these conditions, it is very difficult to measure scotopic ERG responses because the intermittently repeated flashing lights abrogate the dark adaptation that is necessary for scotopic ERG recordings. Because of such technical difficulties, we were not practically able to measure scotopic ERG responses in our current study. AAV-Crx also partially restored outer segment formation in the *Crx* KO mice. This result not only confirms that AAV transduction into the P0 retina is a useful method for *in vivo* retinal gene transfer but also suggests that gene

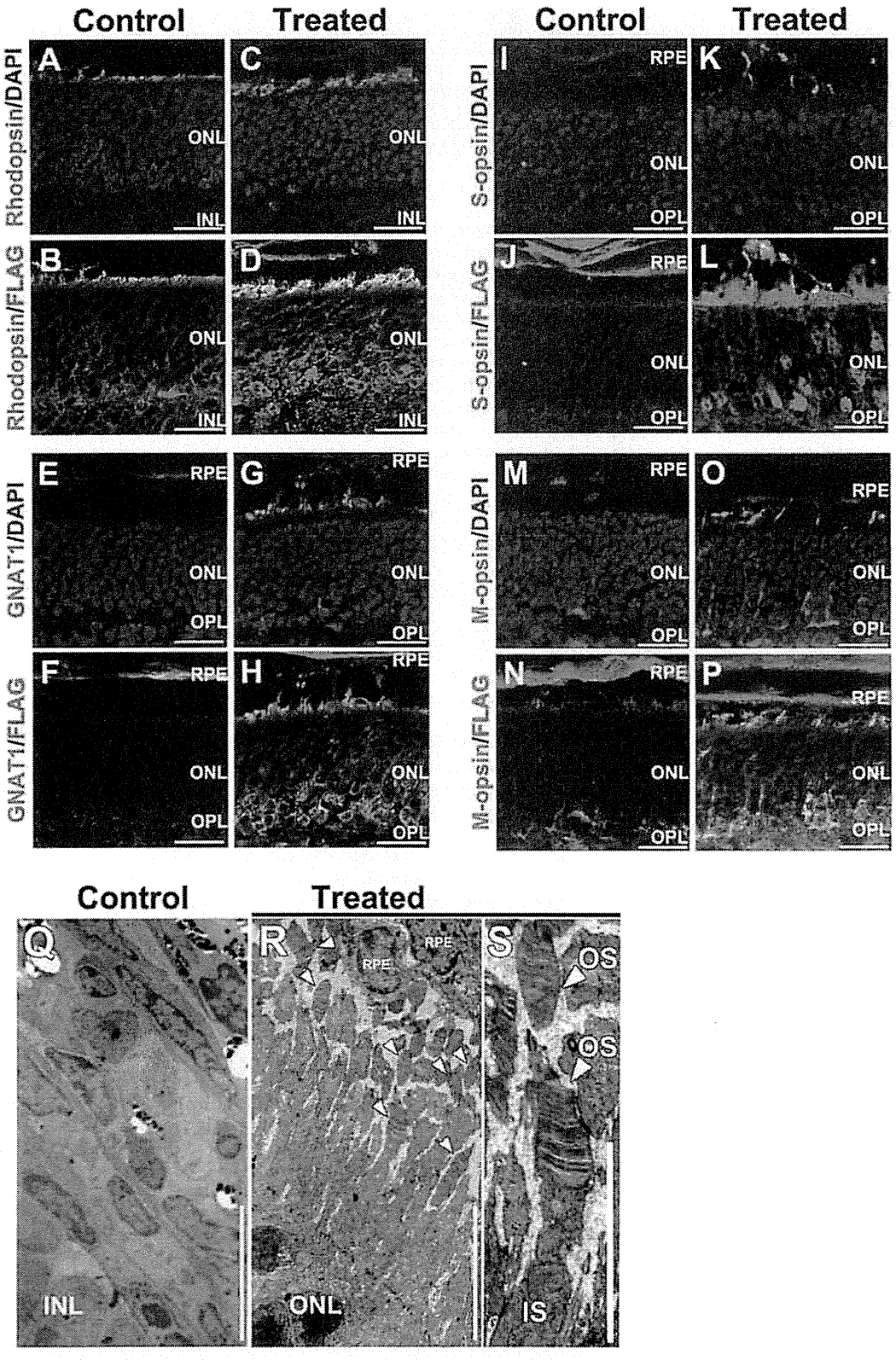

Figure 4. Histological analyses of the *Crx* KO retina transduced with AAV-Crx. (A–P) Immunostaining of the *Crx* KO retinas three weeks after AAV-Crx treatment with outer segment makers of rod photoreceptor (A–H) and cone photoreceptor cells (I–P). Scale bars represent 20 μm (A–P). (Q–

S) Transmission electron microscopy analysis of retinas fifteen weeks after AAV-Crx treatment. (Q and R) In control retinas, no photoreceptor cell was observed (Q). In AAV-Crx-treated retinas, some outer segment structures were observed (R). (S) An enlarged image of outer segments in AAV-Crx-treated retinas. Arrowheads indicate outer segment containing disk lamina. Scale bars represent 7.5 μm (Q and R) and 5 μm (S). RPE: retinal pigment epithelium, ONL: outer nuclear layer, OPL: outer plexiform layer, INL: inner nuclear layer, GCL: ganglion cell layer. OS: outer segment, IS: inner segment.
doi:10.1371/journal.pone.0054146.g004

therapy for human retinal diseases caused by *Crx* mutations is possible. In addition, this is the first report on AAV-mediated rescue for mice with mutations of a transcription factor regulating photoreceptor development and related to human photoreceptor degeneration. *Nrl*, *Nr2e3*, and *Otx2* also play crucial roles in photoreceptor development through transcriptional regulation of photoreceptor genes [1,23,24,25]. The mutations of these genes in humans are associated with several types of retinal degeneration (RetNet: https://sph.uth.tmc.edu/retnet/home.htm). Our current result suggests that human retinal degenerations caused by the mutations in these transcription factors can be restored by AAV-mediated gene therapy. This possibility will be examined by AAV-mediated rescue of mice with these gene mutations in the future.

Materials and Methods

Animals

For the evaluation of the tropism of AAVs *in vivo*, we used ICR mice (Charles River). The *Crx* KO mice were generated as described in our previous study [10]. All procedures conformed to the ARVO statement for the Use of Animals in Ophthalmic and Vision Research, and these procedures were approved by the Institutional Safety Committee on Recombinant DNA Experiments and the Animal Research Committee of Osaka Bioscience Institute (approval ID 10-401) and Institute for Protein Research, Osaka University (approval ID 24-05-0). Mice were housed in a temperature-controlled room with a 12-hour light/dark cycle. Fresh water and rodent diet were available at all times.

Plasmid Constructs

For the production of AAV-CAG-mCherry and AAV2/5-Crx2kb-Flag-Crx, we constructed *pAAV-CAG-mCherry* and *pAAV-Crx2kb-Flag-Crx*, respectively. The *CAG* promoter used in this study was previously described [26]. To produce *pAAV-CAG-mCherry*, we initially constructed *pCAGGS-mCherry*. We cut *pAAV-U6-shLhx2-CMV-mCherry* [27] with *NheI* and *NotI* and inserted the *mCherry* fragment into *pCAGGS* digested *EcoRI* and *NotI* using a *NheI/EcoRI* linker. Finally, to produce *pAAV-CAG-mCherry*, we obtained the *CAG-mCherry* fragment by cutting *pCAGGS-mCherry* with *SalI* and *BglII*, and inserted its fragment into *pAAV-IRES-hrGFP* (Agilent technologies) digested with *NotI* and *BglII* using a *NotI/SalI* linker DNA. To produce *pAAV-Crx2kb-Flag-Crx*, we initially constructed *pCRX(2K)-Flag-Crx-βgal* [17]. The *Flag-mouseCrx* fragment was obtained by cutting *pcDNA3-Flag-Crx* [28] with *XhoI* and *XbaI*. We inserted it into *pCRX(2K)-βgal* digested with *KpnI* and *NheI* using an *XhoI/SalI* linker DNA and obtained *pCRX(2K)-Flag-Crx-βgal*. We next constructed *pCRII-bluntI-Crx2kb-Flag-Crx*. We first obtained the *Crx2kb-Flag-Crx* fragment by cutting *pCRX(2K)-Flag-Crx-βgal* with *SalI* and *XhoI*. We inserted it into *pCRII-bluntI* digested with *XhoI*, and obtained *pCRII-bluntI-Crx2kb-Flag-Crx*. Finally, to produce *pAAV-Crx2kb-Flag-Crx*, we cut *pCRII-bluntI-Crx2kb-Flag-Crx* with *NotI* and *XhoI*, and inserted its fragment using a *NotI/BglII* linker into *pAAV-IRES-hrGFP* (Agilent technologies) digested with *NotI* and *BglII*.

AAV Production

AAV was produced by triple transfection of an AAV vector plasmid, an adenovirus helper plasmid, and an AAV helper plasmid (*pAAV2/1*, *pAAV-RC* [Agilent technologies], *pXR5*, *pAAV2/8*, *pAAV2/9*, *pAAV2/rh10*, and *pEEV2/11*) into AAV-293 cells by the calcium phosphate method. The cells were harvested at 72 hours after transfection, and lysed by four freeze-and-thaw cycles. The supernatant was collected by centrifugation, and treated with Benzonase nuclease (Novagen) to eliminate cellular DNA/RNA and excess plasmid DNAs. This virus preparation was used for subretinal administration. A titer of each AAV (in vector genomes (VG)/mL) was determined by qPCR using SYBR GreenER Q-PCR Super Mix (Invitrogen) and Thermal Cycler Dice Real Time System Single MRQ TP870 (Takara). The primers used for AAV titrations are listed in Table S1. The titers of all serotypes of AAV-CAG-mCherry used in this study were adjusted to approximately 2×10^{12} VG/mL. The titer of AAV2/5-Crx2kb-Flag-Crx used in the *Crx* KO rescue experiment is 2.6×10^{12} VG/mL.

Subretinal Injection

Subretinal injection of AAV was performed as described elsewhere [3,29]. P0 mice were anesthetized by chilling on ice, the eye was opened by cutting along the fused junctional epithelium where the two eyelids come together, and a small incision was made with a 30-gauge needle in the sclera near the junction with the cornea. 0.4 μL of an AAV preparation was injected into the subretinal space through the incision using an Ito micro syringe (Ito Corporation) with a 33-gauge blunt-ended needle under a dissecting microscope. Fast Green dye was added to AAV preparations at a final concentration of 0.1% as a tracer to confirm that the AAV preparations were injected into the subretinal space [29]. For histological analyses, we only used retinas in which the dye in the AAV preparation was confirmed to be evenly distributed and which were without severe damage caused by the injection process.

Immunostaining

For immunohistochemistry, 14 μm thick retina sections were washed twice in phosphate-buffered saline (PBS), and permeabilized with 0.1% Triton X-100 (wt/vol) in PBS, then incubated with PBS containing 4% donkey serum (vol/vol) for 1 h to block samples. The samples were incubated with a primary antibody at 4°C overnight. After washing with PBS, these samples were incubated with secondary antibodies at 25°C for 1 hour. In the current study, we also used the following primary antibodies: anti-RHODOPSIN antibody (1:10000, O4886, Sigma) as a rod photoreceptor cell marker, anti-S-OPSIN antibody (1:500, sc-14363, Santa Cruz) as a cone photoreceptor cell marker, anti-CALB1 antibody (1:1000, PC253L, Sigma) as a horizontal cell marker, anti-CHX10 antibody (1:200, MBL) as a bipolar cell marker, anti-PAX6 antibody (1:100, DSHB) as an amacrine cell maker, anti-BRN3B antibody (1:100, sc-6026, Santa Cruz) as a ganglion cell maker, anti-S100β antibody (1:100, S-2532, Sigma) as Müller glial cell marker, anti-GNAT1 antibody (1:3000, sc-389, Santa Cruz), anti-M-OPSIN antibody (1:500, AB5402, Chemicon), and anti-FLAG antibody (1:1000, F1804, Sigma). The

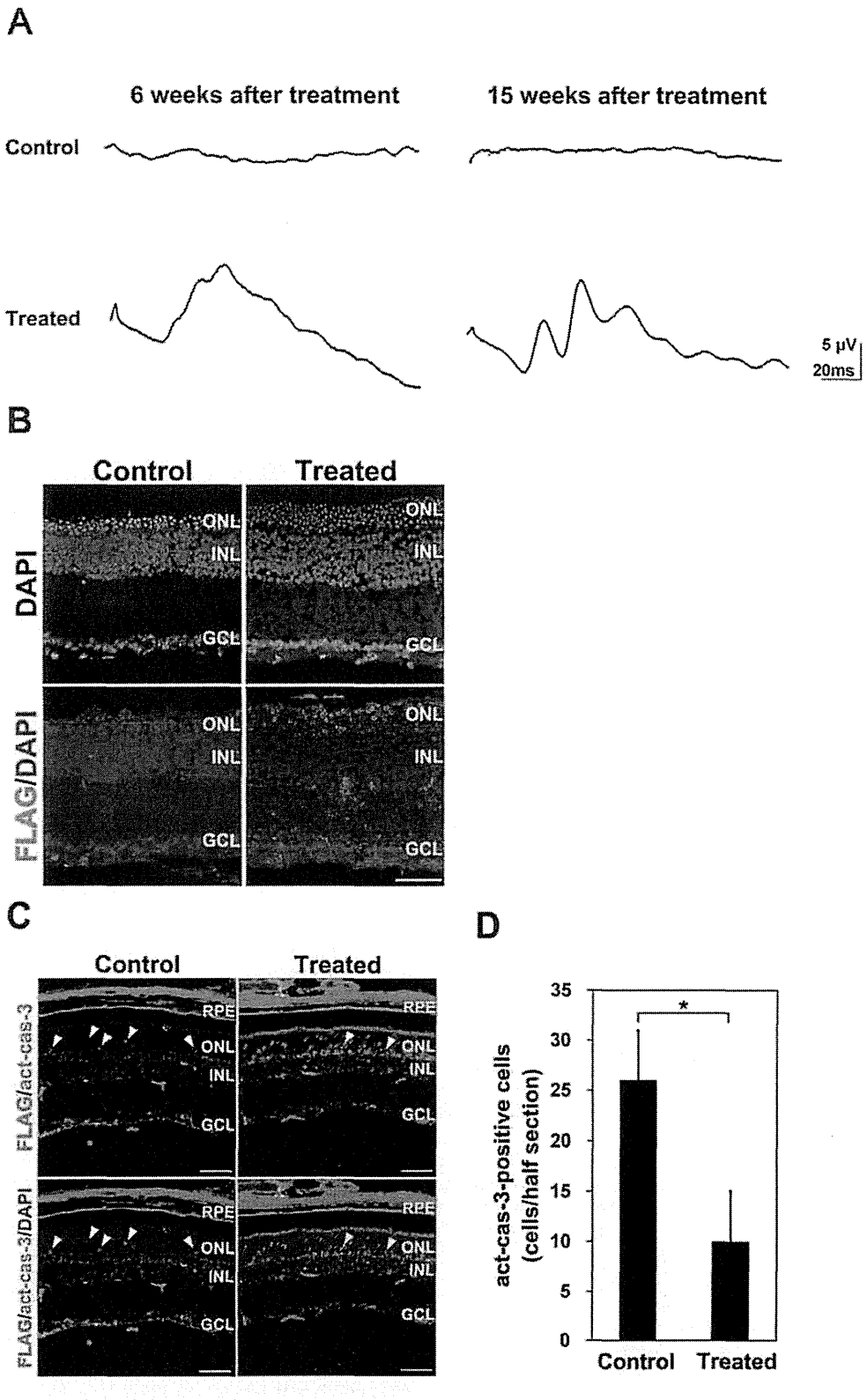

Figure 5. Restoration of function and morphology in the *Crx* KO retina treated with AAV-Crx. (A) Representative ERGs recorded at six and fifteen weeks after AAV-Crx treatment. ERG responses averaged from one hundred 1.0 log cd-s/m^2 stimuli. The mice used for ERG recordings were independently prepared between the two time points. At both six and fifteen weeks after AAV treatment, all three of the control eyes from different

mice showed no ERG response, while two of the three treated eyes from different mice showed significant responses. (B) Immunostaining of FLAG-CRX in the retinas at fifteen weeks after AAV-Crx treatment. (C and D) Immunostaining of active-caspase-3 and FLAG-CRX in *Crx* KO retinas three weeks after AAV-Crx treatment (C). The number of active-caspase-3-positive cells (D, Control retinas: n = 3 from three different mice and AAV-treated *Crx* KO retinas: n = 4 from four different mice). Arrowheads indicate active-caspase-3-positive cells. Scale bar represents 50 μm. Error bar represents the SD from the means of three control retinas and four treated retinas. $^{*}p<0.05$. RPE: retinal pigment epithelium, ONL: outer nuclear layer, INL: inner nuclear layer, GCL: ganglion cell layer.
doi:10.1371/journal.pone.0054146.g005

following secondary antibodies were also used: Alexa Fluor 488-conjugated anti-mouse IgG (1:300, A11001, Invitrogen), Alexa Fluor 488-conjugated anti-rabbit IgG (1:300, A11008, Invitrogen), Alexa Fluor 488-conjugated anti-goat IgG (1:300, A11055, Invitrogen), Cy3-conjugated anti-mouse IgG (1:300, 715-165-150, Jackson), and Cy3-conjugated anti-rabbit IgG (1:300, 705-165-147, Jackson). For immunostaining of the whole retina, each retina was gently peeled off from the sclera, rinsed in PBS, and fixed with 4% paraformaldehyde (wt/vol) in PBS for 1.5 h. The retinas were permeabilized by incubation in 0.1% Triton X-100 in PBS (PBST) for 30 min. After washing in PBST, samples were blocked with 4% donkey serum in PBST for 1 h. The retinas were then immunostained with primary antibodies against mCherry (1:1000, 632496, Clontech) at 4°C overnight. After washing in PBST, reactions with a Cy3-conjugated anti-rabbit IgG secondary antibody were performed overnight at 4°C.

Quantification of Infection Efficiency

AAV-CAG-mCherry-injected retinas were co-immunostained with cell type-specific markers for each retinal cell shown above and an anti-mCherry antibody. We counted the number of marker-positive cells and marker/mCherry double-positive cells according to cell types for the calculation of infection efficiencies. We used high-resolution confocal images of retinal sections along the z-axis (2.0 μm) taken with the LSM 700 (Zeiss, 20× or 40× objectives) to count cell numbers and measure infection efficiencies for rod and cone photoreceptor, bipolar, Müller glial, and amacrine cells. Since horizontal and ganglion cells in the confocal images (20×) are small in number (<10 cells), it is very difficult to accurately calculate the infection efficiencies of these cell types in contrast to other cell types. Thus, we counted the whole cell numbers seen through a fluorescence microscope for calculating the infection efficiencies of these cell types. We used three retinas from three different mice and counted 100–200 rod photoreceptor and amacrine cell marker-positive cells, 30–45 cone photoreceptor cell marker-positive cells, 30–100 horizontal and ganglion cell marker-positive cells, 40–140 bipolar cell marker-positive cells, and 30–60 Müller glial cell marker-positive cells for measuring infection efficiency for each retinal cell type. To show that AAV infection diffused throughout the retina, infection efficiencies in rod photoreceptor cells were calculated in the three areas, which are central, middle and peripheral areas to optic nerve head at the side uninjured by injection. Infection efficiencies in cone photoreceptor, bipolar, amacrine, and Müller glial cells were calculated in the central area. Infection efficiencies in horizontal and ganglion cells were calculated throughout the retina of the side uninjured by injection.

Table 1. Quantitative analysis of ERG amplitudes in control and AAV-Crx treated eyes.

	a-wave amplitudes	b-wave amplitudes
Control eye (6 weeks)		
1	0	0
2	0	0
3	0	0
AAV-treated eye (6 weeks)		
1	4.3	9.0
2	1.4	12.1
3	0	0
Control eye (15 weeks)		
1	0	0
2	0	0
3	0	0
AAV-treated eye (15 weeks)		
1	4.0	13.0
2	3.4	11.0
3	0	0

doi:10.1371/journal.pone.0054146.t001

Western Blot Analysis

Western blot analysis was performed as described previously [27]. The membrane was incubated with an anti-FLAG antibody (1:1000, F1804, Sigma). The membrane was then incubated with a horseradish peroxidase–conjugated goat antibody against mouse IgG (1:10000, Zymed). For the secondary immunoreaction, the PVDF membrane was incubated with WB Stripping Solution (Nacalai Tesque) to remove antibodies, and blocked again with 5% skim milk (wt/vol) in TBS. Further immunoblots were performed using a mouse antibody against β-actin (ACTB, 1:5000, Sigma).

RT-qPCR

The mouse retinas were harvested and dissected at 3 weeks after injection. Total RNA (1 μg) from the retina was isolated using TRIzol reagent (Invitrogen) and converted to cDNA using Superscript II Reverse Transcriptase (Invitrogen). Real time PCR was performed using SYBR GreenER Q-PCR Super Mix (Invitrogen) and Thermal Cycler Dice Real Time System Single MRQ TP870 (Takara) according to the manufacturer's instructions. Quantification was performed by Thermal Cycler Dice Real Time System software version 2.0 (Takara). The primer sequences used for qPCR are listed in Table S1.

ERG Recordings

Mice were anesthetized with an intramuscular injection of 80 mg/kg ketamine and 16 mg/kg xylazine. Pupils were dilated with topical 0.5% tropicamide and 0.5% phenylephrine HCl, and the mice were placed on a heating pad for the duration of the ERG recordings. ERGs were recorded with a gold wire loop placed on the cornea anesthetized with 1% tetracaine. A gold wire electrode was placed on the sclera 1 mm from the temporal limbus as the reference electrode. The mice were placed in a Ganzfeld bowl and 100 stroboscopic stimuli of 1.0 log cd-s/m^2 (PS33 Plus; Grass Telefactor) were averaged with a repetition rate of 1 sec to record the ERGs. Signals were amplified and bandpass filtered between 1 and 1000 Hz (Power Lab; AD Instruments, Castle Hill,

Australia). Amplitudes of both a- and b-waves were quantified from photopic ERG responses.

Transmission Electron Microscopy

Specimens for transmission electron microscopy were prepared in the following manner. Eyes were enucleated from anaesthetized mice. Following the removal of anterior segment, each posterior eyecup was fixed with 2% glutaraldehyde and 2% paraformaldehyde in a cacodylate-based buffer adjusted at pH 7.4. After fixation with 1% osmium tetraoxide for 90 min, the retinas were dehydrated through a graded series of ethanol (50%–100%) and n-butylglycidylether. Finally, they were embedded in epoxy resin. Ultrathin sections were cut on an ultramicrotome (Ultracut E, Reichert-Jung, Vienna, Austria), and stained with uranyl acetate and lead citrate. Retinas were observed by transmission electron microscope (1200EX, JEOL, Japan).

Statistical Analysis

Statistical significance was calculated with a Student's t test. A value of $p<0.05$ was taken to be statistically significant. Data are presented as means ± SD.

Supporting Information

Table S1 Primer sequences. Primers for qPCR analysis. (XLS)

Acknowledgments

We thank J. Johnston for the *pAAV2/1*, *pXR5*, *pAAV2/8*, *pAAV2/9*, and *pAAV2/rh10* vectors, and S. Mori for the *pEEV2/11* vector. We thank Y. Chérrase for help in producing the AAV. We thank Y. Omori, A. Onishi, Y. Muranishi, T. Chaya and S. Irie for critical comments and technical advice, and A. Tani, M. Kadowaki, A. Ishimaru, H. Tsujii, Y. Saioka, H. Abe, and S. Kennedy for technical assistance.

Author Contributions

Conceived and designed the experiments: TF SW RS. Performed the experiments: SW RS SU TK TH. Analyzed the data: SW TF RS SU TH. Contributed reagents/materials/analysis tools: TF SU TH. Wrote the paper: SW TF.

References

1. Omori Y, Katoh K, Sato S, Muranishi Y, Chaya T, et al. (2011) Analysis of transcriptional regulatory pathways of photoreceptor genes by expression profiling of the otx2-deficient retina. PLoS One 6: e19685.
2. Gamsiz ED, Ouyang Q, Schmidt M, Nagpal S, Morrow EM (2012) Genome-wide transcriptome analysis in murine neural retina using high-throughput RNA sequencing. Genomics 99: 44–51.
3. Matsuda T, Cepko CL (2004) Electroporation and RNA interference in the rodent retina in vivo and in vitro. Proc Natl Acad Sci U S A 101: 16–22.
4. Bostick B, Ghosh A, Yue Y, Long C, Duan D (2007) Systemic AAV-9 transduction in mice is influenced by animal age but not by the route of administration. Gene Ther 14: 1605–1609.
5. Surace EM, Auricchio A, Reich SJ, Rex T, Glover E, et al. (2003) Delivery of adeno-associated virus vectors to the fetal retina: impact of viral capsid proteins on retinal neuronal progenitor transduction. J Virol 77: 7957–7963.
6. Auricchio A, Kobinger G, Anand V, Hildinger M, O'Connor E, et al. (2001) Exchange of surface proteins impacts on viral vector cellular specificity and transduction characteristics: the retina as a model. Hum Mol Genet 10: 3075–3081.
7. Allocca M, Mussolino C, Garcia-Hoyos M, Sanges D, Iodice C, et al. (2007) Novel adeno-associated virus serotypes efficiently transduce murine photoreceptors. J Virol 81: 11372–11380.
8. Furukawa T, Morrow EM, Cepko CL (1997) Crx, a novel otx-like homeobox gene, shows photoreceptor-specific expression and regulates photoreceptor differentiation. Cell 91: 531–541.
9. Chen S, Wang QL, Nie Z, Sun H, Lennon G, et al. (1997) Crx, a novel Otx-like paired-homeodomain protein, binds to and transactivates photoreceptor cell-specific genes. Neuron 19: 1017–1030.
10. Furukawa T, Morrow EM, Li T, Davis FC, Cepko CL (1999) Retinopathy and attenuated circadian entrainment in Crx-deficient mice. Nat Genet 23: 466–470.
11. Freund CL, Gregory-Evans CY, Furukawa T, Papaioannou M, Looser J, et al. (1997) Cone-rod dystrophy due to mutations in a novel photoreceptor-specific homeobox gene (CRX) essential for maintenance of the photoreceptor. Cell 91: 543–553.
12. Swain PK, Chen S, Wang QL, Affatigato LM, Coats CL, et al. (1997) Mutations in the cone-rod homeobox gene are associated with the cone-rod dystrophy photoreceptor degeneration. Neuron 19: 1329–1336.
13. Sohocki MM, Sullivan LS, Mintz-Hittner HA, Birch D, Heckenlively JR, et al. (1998) A range of clinical phenotypes associated with mutations in CRX, a photoreceptor transcription-factor gene. Am J Hum Genet 63: 1307–1315.
14. Freund CL, Wang QL, Chen S, Muskat BL, Wiles CD, et al. (1998) De novo mutations in the CRX homeobox gene associated with Leber congenital amaurosis. Nat Genet 18: 311–312.
15. Glove TJ, Sena-Esteves M, Eldred WD (2010) Transduction of the inner mouse retina using AAVrh8 and AAVrh10 via intravitreal injection. Exp Eye Res 91: 652–659.
16. Mori S, Wang L, Takeuchi T, Kanda T (2004) Two novel adeno-associated viruses from cynomolgus monkey: pseudotyping characterization of capsid protein. Virology 330: 375–383.
17. Furukawa A, Koike C, Lippincott P, Cepko CL, Furukawa T (2002) The mouse Crx 5'-upstream transgene sequence directs cell-specific and developmentally regulated expression in retinal photoreceptor cells. J Neurosci 22: 1640–1647.
18. Koike C, Nishida A, Akimoto K, Nakaya MA, Noda T, et al. (2005) Function of atypical protein kinase C lambda in differentiating photoreceptors is required for proper lamination of mouse retina. J Neurosci 25: 10290–10298.
19. Hsiau TH, Diaconu C, Myers CA, Lee J, Cepko CL, et al. (2007) The cis-regulatory logic of the mammalian photoreceptor transcriptional network. PLoS One 2: e643.
20. Morrow EM, Furukawa T, Raviola E, Cepko CL (2005) Synaptogenesis and outer segment formation are perturbed in the neural retina of Crx mutant mice. BMC Neurosci 6: 5.
21. Cepko CL, Austin CP, Yang X, Alexiades M, Ezzeddine D (1996) Cell fate determination in the vertebrate retina. Proc Natl Acad Sci U S A 93: 589–595.
22. Gao G, Vandenberghe LH, Wilson JM (2005) New recombinant serotypes of AAV vectors. Curr Gene Ther 5: 285–297.
23. Mears AJ, Kondo M, Swain PK, Takada Y, Bush RA, et al. (2001) Nrl is required for rod photoreceptor development. Nat Genet 29: 447–452.
24. Chen J, Rattner A, Nathans J (2005) The rod photoreceptor-specific nuclear receptor Nr2e3 represses transcription of multiple cone-specific genes. J Neurosci 25: 118–129.
25. Nishida A, Furukawa A, Koike C, Tano Y, Aizawa S, et al. (2003) Otx2 homeobox gene controls retinal photoreceptor cell fate and pineal gland development. Nat Neurosci 6: 1255–1263.
26. Niwa H, Yamamura K, Miyazaki J (1991) Efficient selection for high-expression transfectants with a novel eukaryotic vector. Gene 108: 193–199.
27. Sanuki R, Onishi A, Koike C, Muramatsu R, Watanabe S, et al. (2011) miR-124a is required for hippocampal axogenesis and retinal cone survival through Lhx2 suppression. Nat Neurosci 14: 1125–1134.
28. Muranishi Y, Terada K, Inoue T, Katoh K, Tsujii T, et al. (2011) An Essential Role for RAX Homeoprotein and NOTCH-HES Signaling in Otx2 Expression in Embryonic Retinal Photoreceptor Cell Fate Determination. J Neurosci 31: 16792–16807.
29. de Melo J, Blackshaw S (2011) In vivo electroporation of developing mouse retina. J Vis Exp 52: pii 2847.

厚生労働省　難病・がん等疾患分野の医療の実用化研究事業

次世代シークエンサーを用いたエクソーム配列解析による黄斑ジストロフィーの原因遺伝子と発症機序の解明

（H23-実用化（難病）- 一般-006）

平成24年度　総括研究報告書

岩田　岳

平成25年5月

EXPERIMENTAL MEDICINE
実験医学 月刊

別　刷

羊土社
〒101-0052
東京都千代田区神田小川町2-5-1
TEL：03-5282-1211（代表）　FAX：03-5282-1212
E-mail：eigyo@yodosha.co.jp
URL：http://www.yodosha.co.jp/

視力・色覚を司る黄斑の生理機能と黄斑変性の分子メカニズム

岩田　岳

ヒトは情報の8割を視覚に依存すると考えられており，眼は重要な感覚器官である．眼の中でも特に網膜の中心に位置して視細胞が高い密度で存在する黄斑は視力と色覚を司る重要な部位である．黄斑には周辺網膜に存在する視神経や毛細血管がなく，凹型構造となって視細胞が網膜表明に近づくことにより，感度がより高くなっている．この特殊な構造こそが，逆に組織的な脆弱性を生み，多くの黄斑疾患の病巣となっている．

キーワード：網膜，黄斑，視細胞，中心窩，加齢黄斑変性，オカルト黄斑ジストロフィー

はじめに

角膜，水晶体，そして硝子体を通過した光は網膜に結像するが，光を感じる視細胞は網膜内に均一に存在するわけではなく，黄斑に集中している（図1A）．黄斑の中心には感度は低いが色覚を司る錐体細胞（cone）が集中し，そのすぐ周辺には色覚はないが感度の高い桿体細胞（rod）が取り巻く．黄斑疾患には浮腫，剥離，嚢腫，萎縮，変性などのさまざまな障害の形態があり，複数の要因によって発症するが，そのなかでも世界的に有病率の高い難治性疾患（厚生労働省認定）として加齢黄斑変性（age-related macular degeneration）がある．米国では中途失明の原因として第1位であり，日本でも急速な高齢化によって患者数が増加している．加齢黄斑変性は遺伝子，加齢，喫煙，肥満，青色光など複数の要因によって発症することが疫学調査によって明らかにされており，この10年間に発症機序が徐々に明らかになってきた．さらに，黄斑の変性症としては強い近視に起きやすい新生血管黄斑症，若年層にも起きる突発性脈絡膜新生血管，そして遺伝的要因のみで発症する黄斑ジストロフィー（先天性黄斑変性）がある．本稿ではこれらの黄斑変性症のなかでも多因子疾患の加齢黄斑変性と，黄斑部の錐体機能のみが著しく低下するメンデル遺伝形式の黄斑ジストロフィー（macular dystrophy）の一種であるオカルト黄斑ジストロフィー（occult macular dystrophy：三宅病）の原因遺伝子解明についてご紹介する．

黄斑部の組織構造と環境

厚さわずか0.1～0.3 mmの網膜は感覚網膜9層と網膜色素上皮細胞から構成され，感覚網膜には神経細胞の視細胞，双極細胞，水平細胞，アマクリン細胞，神経節細胞に加えて，グリア系細胞と血管系細胞が存在する．検眼鏡的には黄斑は視神経乳頭の中心から4 mm耳側に位置し，直径1.5～2.0 mmの黄色を呈する円周を指し，この中心の直径約0.35 mm（中心窩）は神経節細胞や内顆粒層が周囲に移動して浅く陥凹し，

Visual function of the macula and molecular mechanism of the macular diseases
Takeshi Iwata：Division of Molecular & Cellular Biology, National Institute of Sensory Organs, National Hospital Organization Tokyo Medical Center〔国立病院機構東京医療センター臨床研究センター（感覚器センター）分子細胞生物学研究部〕

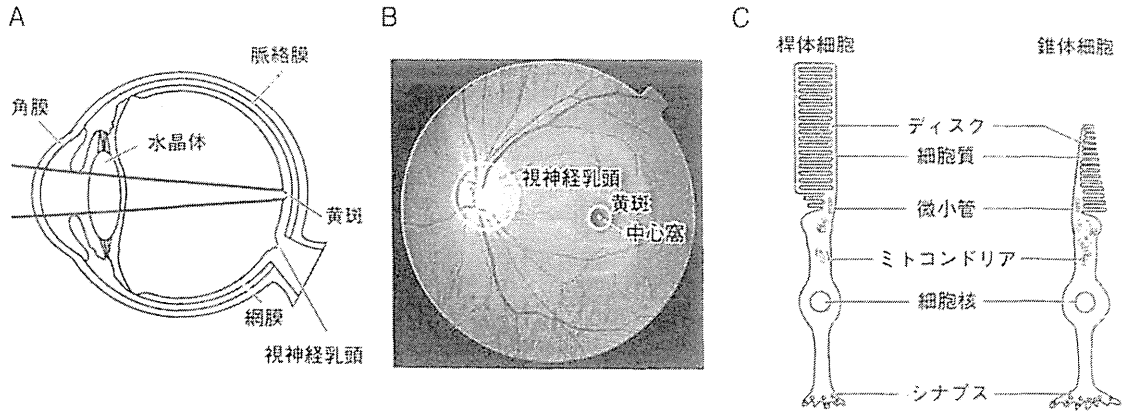

図1　眼球の構造と視細胞

A）角膜と水晶体を通過した光は黄斑で焦点を結ぶ．B）ヒトの眼底像．C）視細胞（桿体細胞と錐体細胞）の構造．円盤状のディスク上に桿体細胞ではロドプシン，錐体細胞では赤，緑，青のいずれかのオプシンが存在する．中心窩では主に赤と緑のオプシンを発現する錐体細胞が集中して存在し，少し外れると桿体細胞数が顕著に増加する

無血管な領域であり，錐体細胞のみが網膜の表面に位置する構造になっている（図1B，C）．黄斑は魚類にはじまり，爬虫類，鳥類へと受け継がれたが，哺乳類の登場時にはいったん消失し，霊長類で再現したことが知られている．霊長類の周辺網膜では神経節細胞－双曲細胞－視細胞のシナプス様式は1：多：多々となっているのに対し，中心小窩（中心窩の中央部分）では1：1：1となっており，ここでは最高の視力が確保されるが，少しでも中心小窩からずれると急激に視力は低下する．錐体細胞は桿体細胞に比べて細胞当たりのエネルギー代謝が約8倍異なり，ミトコンドリアの数も細胞当たりでは20倍も異なることが知られている[1]．すなわち黄斑の中心は無血管でありながら活発に代謝・機能を維持しなければならない環境になっており，栄養や酸素の供給が不足すると容易に機能が低下する危険性がある．

2 加齢黄斑変性と全ゲノム相関解析

視細胞では，その生理機能を維持するために血管の豊富な脈絡膜との間で酸素，栄養素，老廃物の交換が盛んに行われている．網膜色素上皮細胞は視細胞と脈絡膜の間を隔てるように位置し，分子輸送や視細胞の貪食作用，そして各種生体因子の分泌機能などによって網膜の恒常性を維持している．網膜色素上皮細胞の老化によってこれらの機能が低下すると細胞内に細胞毒性のあるリポフスチンや基底膜側に黄色のドルーゼン※1が蓄積する．これらの蓄積はやがて網膜色素上皮細胞の萎縮（萎縮型加齢黄斑変性）や黄斑部における血管新生（滲出型加齢黄斑変性）となって，視細胞が障害され，中心視力が著しく低下する．

近年，遺伝子多型（SNP）チップを用いた多因子疾患の全ゲノム相関解析（genome wide association study：GWAS）が盛んに行われているが，加齢黄斑変性はその最初の成功例である．アメリカ人患者を対象にしたマイクロサテライトマーカーによる全ゲノム相関解析において強い相関のあった領域については，SNPチップによって染色体1番に存在する補体H因子の遺伝子多型が疾患と強く相関することが報告された[2,3]．このなかでも特にH因子のY402H（rs1061170）の遺伝子多型は白人，ヨーロッパ系インド人において多くの患者について相関したのに対して，日本人や中国人ではY402Hの相関は観察されず，I62V（rs800292）が一部の患者で相関する程度であった[4,5]．今後の他のアジア人

※1　ドルーゼン
ブルッフ膜[3]と網膜色素上皮細胞の間に蓄積する黄色あるいは白色の物質．その構成成分は脂質，補体，アミロイド，クリスタリンなど多岐にわたる

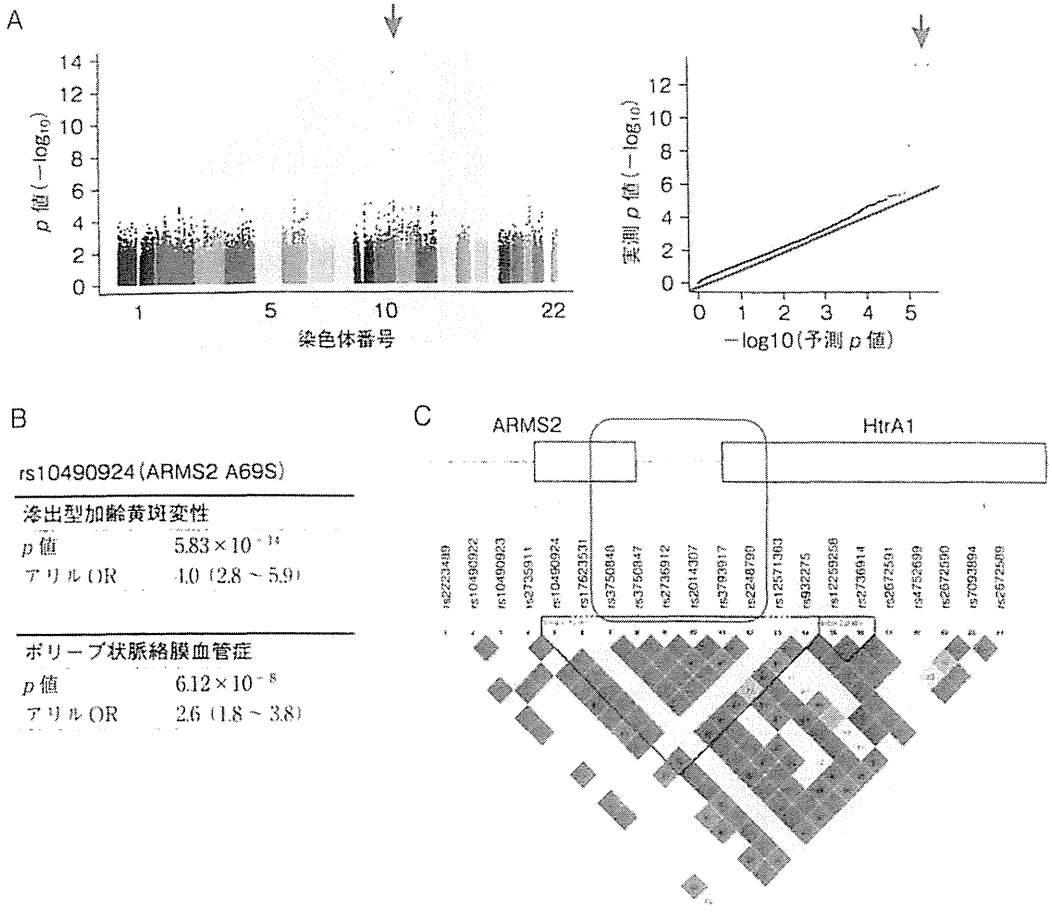

図2　日本人滲出型加齢黄斑変性の全ゲノム相関解析
A）全ゲノム相関解析によって染色体10番に強い相関が観察された（→）．B）この領域のタグSNP rs10490924の加齢黄斑変性およびポリープ状脈絡膜血管症におけるp値とオッズ比（OR）．C）rs10490924と連鎖不平衡（linkage disequilibrium）を共有する領域はARMS2からHtrA1の2遺伝子にまたがり，いずれの遺伝子が疾患に関与するのか研究されている（Aは文献9より転載）

※2　補体副経路
副経路は病原体表面で直接C3の分解が行われることで開始する補体活性経路の1つ．肝臓でつくられたC3は血液中でC3aとC3bに分解される．C3bは病原体の細胞膜に結合し，これにB因子が結合する．さらにこの複合体はD因子によって分解され，BaおよびC3転換酵素Bbとなる．C3bBb複合体はC3をさらにC3aとC3bに分解し，病原体表面のC3bBbは増加する．C3b複合体はC3bBbC3bとなり，これはC5をC5aとC5bに分解し，C5b，C6，C7，C8，C9からなる複合体は細胞膜障害性複合体（membrane attack complex：MAC）を形成し，病原体の細胞膜に穴を開け，浸透圧の変化によって細胞を溶解する．H因子はC3bに結合することで副経路に抑制的に働く．

※3　ブルッフ膜
膠原線維を主体とする無細胞性の層構造．網膜色素上皮と脈絡膜が接する．網膜-脈絡膜間の物質交換の通路となっている．

口におけるH因子の遺伝子多型解析が注目されている．Y402HはH因子の反復配列（short consensus repeats：SCRs）の7番目にあり，C3b，C反応性タンパク質（C-reactive protein），グリコサミノグリカンとの結合部位に位置し，補体副経路[※2]の制御に影響すると考えられる．H因子のノックアウトマウス（*cfh*$^{-/-}$）は視細胞の障害，網膜におけるC3の蓄積，ブルッフ膜[※3]の菲薄化が観察されている[6]．さらに，染色体10番ではLOC387715/ARMS2（age-related maculopathy susceptibility 2）とHtrA1（HtrA serine peptidase 1）

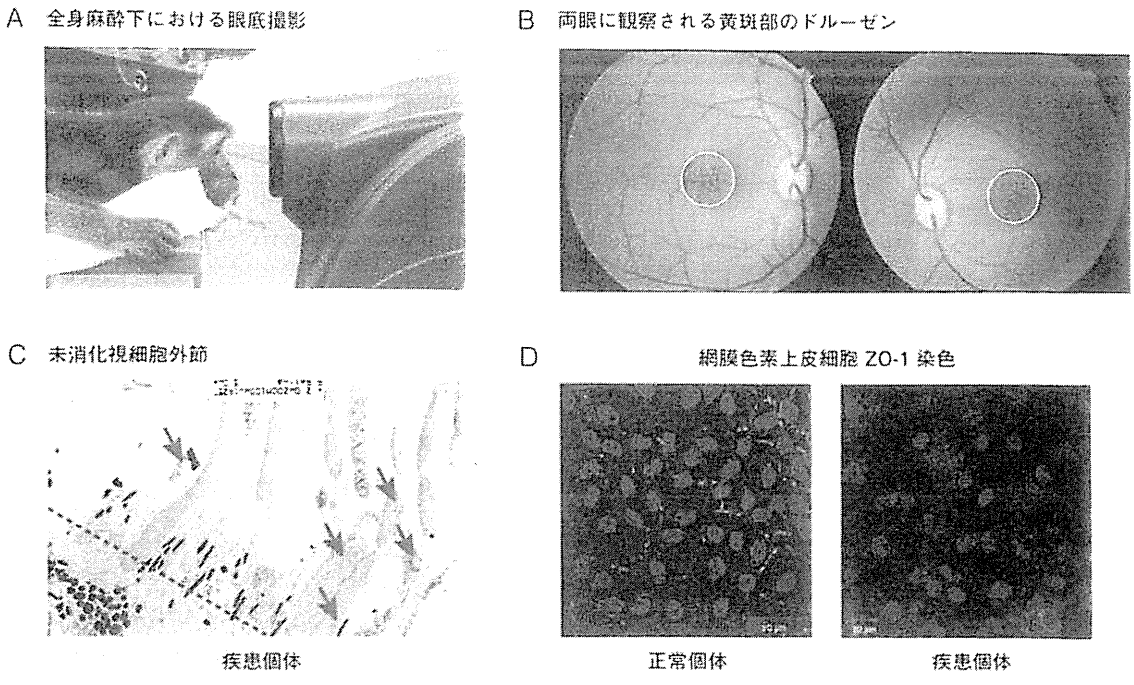

図3 黄斑変性カニクイザルの病理学的解析
A）全身麻酔下においての眼底撮影（医薬基盤研究所霊長類医科学研究センター）．B）疾患個体の眼底像．黄斑部に黄色のドルーゼンが集中して存在する．C）疾患サルの網膜と網膜色素上皮細胞との境界（……）を撮影した電子顕微鏡写真．網膜色素上皮細胞の貪食作用の機能低下によって未消化の桿体細胞（⟶）外節が観察された．D）正常個体と疾患個体の網膜色素上皮細胞の細胞接着機能の観察．ZO-1 染色（緑）によって疾患サルの細胞では接着機能が破綻していることが観察された．青は細胞核（DAPI 染色）

遺伝子領域における遺伝子多型が強く相関した[7]．われわれは日本人に多くみられる滲出型黄斑変性のみを集め，独自に全ゲノム相関解析を行ったところ，染色体1番のCFH領域は相関せず，染色体10番のLOC387715/ARMS2のみが相関することを明らかにした（図2）[8][9]．この領域に存在する2つの遺伝子の片方／両方が加齢黄斑変性のリスクを高めるのか，現時点では明らかにされていない．LOC387715/ARMS2遺伝子はマウスには存在せず，ヒトLOC387715/ARMS2を発現するトランスジェニックマウスを作製したところ血管新生に関する抑制効果が観察されている．また，HtrA1のノックアウトマウスでは高齢でも網膜の形態的な異常は観察されていない．加齢黄斑変性は多因子疾患であることから，その再現にはこれらのマウスに環境的なストレスを加える必要があり，現在実験が行われている．

黄斑変性霊長類モデルの解析

ドルーゼンの蓄積が黄斑を中心に広範囲に及ぶと，これに接する網膜色素上皮細胞は徐々に萎縮し，黄斑部の視細胞も障害されて萎縮型加齢黄斑変性となる．これは脈絡膜から視細胞に向かって黄斑部で血管新生が起こる滲出型加齢黄斑変性と区別される．萎縮型は白人での頻度が高く，滲出型は日本人に多いことが知られている．ドルーゼンの生成メカニズムはまだ十分に解明されていないが，遺伝子多型，視細胞を保護する不飽和脂質（DHA）の光酸化分子に対する自己抗体[10]，アミロイドβの蓄積による補体活性化[11]，サイトメガロウイルス感染による炎症[12][13]，ケモカインの亢進や補体の活性化[14]～[16]など複数の原因が考えられている．このなかでも特に，ドルーゼンや網膜色素上皮細胞に補体の活性化が確認されており，患者の網膜切片の免

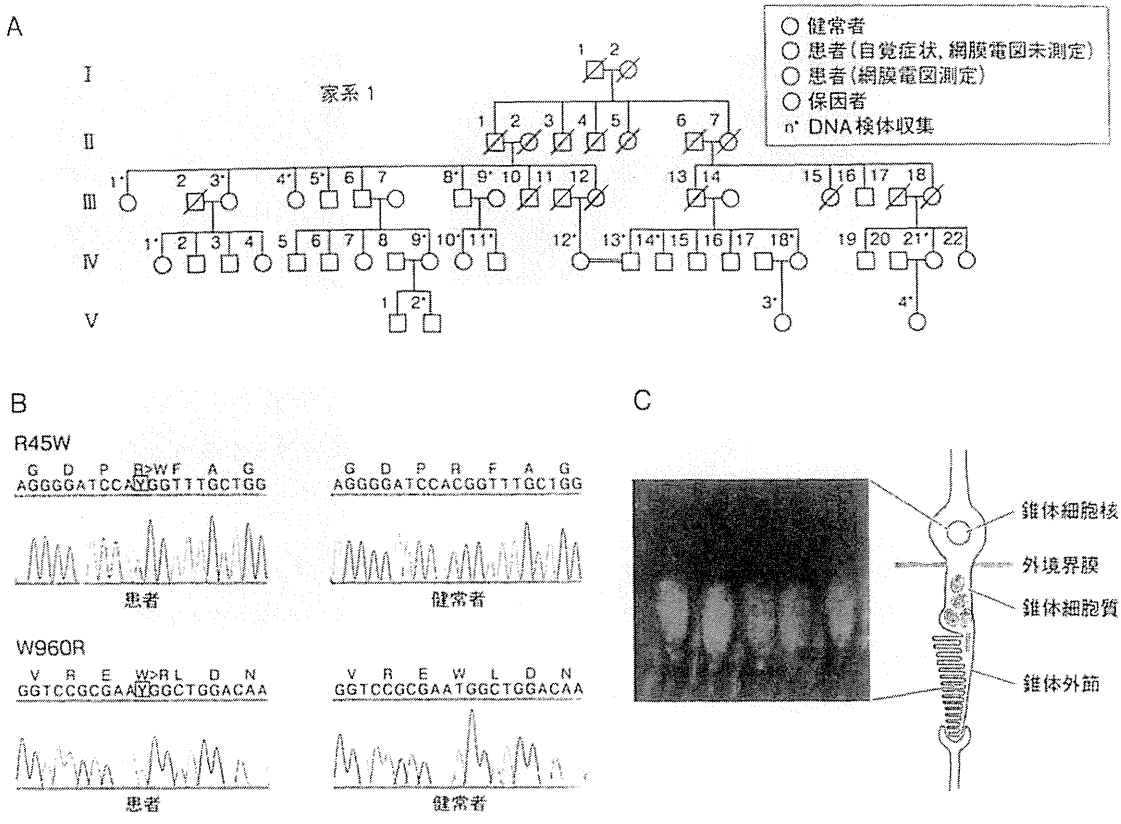

図4　オカルト黄斑ジストロフィーと*RP1L1*遺伝子

A）オカルト黄斑ジストロフィーの家系．この優性遺伝の家系を用いてSNP HiTLink連鎖解析法を行い，8番染色体短腕に連鎖領域がマッピングされた．B）患者に観察された*RP1L1* R45WとW960R遺伝子変異．2つの変異はコントロール876人では検出されなかった．C）RP1L1の免疫染色（緑）．RP1L1のN末端に対して作製された抗体を用いて行われた．視細胞の外境界膜から外節にかけて染色された．赤はロドプシンの免疫染色．桿体細胞の外節が染色されている

疫染色によって補体関連分子の陽性反応が観察されている．萎縮型の患者の一部は滲出型へ移行することが知られているが，その詳細なメカニズムは不明のままである．前述のように，加齢黄斑変性のリスク因子として，遺伝子，加齢に加えて，喫煙，肥満，青色光などが知られている．

さて，以上の事実から補体の活性化を抑制することによって，加齢黄斑変性を治療することが考えられ，多くの補体抑制薬について臨床試験でその薬効が評価されている．黄斑は一部の霊長類と鳥類にしか存在しないために，厳密には一般的な実験動物（マウス，ラット，モルモット）では黄斑に関係する実験はできない．そこでわれわれは独立行政法人医薬基盤研究所霊長類医科学研究センターとの共同研究によって，若年で患者と同成分のドルーゼンを生成する遺伝性の黄斑変性カニクイザルを解析している（図3）[17]．この疾患サルにおいて，ヒトと同様にドルーゼンや網膜色素上皮細胞において補体の活性化が観察されている[18][19]．われわれは補体を抑制することによってドルーゼンの生成を抑制あるいは消滅できるか，C3b抑制薬（Compstatin，John Lambrisによって開発）およびC5b抑制薬（AcPepA，岡田秀親によって開発）の効果を研究中である．先行しているCompstatinについては実験に用いた4頭全頭について，一部のドルーゼンについて消失していく様子が観察された[20]．

オカルト黄斑ジストロフィーの原因遺伝子

オカルト黄斑ジストロフィーは日本人によって発見された数少ない眼疾患の1つであり，黄斑部の錐体細胞のみが障害される病気である[21][22]．われわれは佐渡で発見されたオカルト黄斑ジストロフィーの大家系を調査し（図4A），SNPチップを用いた新しい連鎖解析法（SNP HiTLink，福田陽子と辻 省次によって開発）[23]を用いて解析を行った．その結果，染色体8番短腕にLOD Score 3.7以上の高い連鎖が発見された．連鎖不平衡のrs265309からrs263841までの約10Mbの領域には少なくとも128遺伝子が存在し，このなかから網膜での発現が確認された22の遺伝子が抽出された．さらに，各遺伝子の文献による情報から4つの候補，*MSRA*（methionine sulfoxide reductase A），*GATA4*（GATA binding 4），*PCM1*（pericentriolar material 1），そして*RP1L1*（RP1-like 1）が選択され，これらのダイレクトシークエンスを行った．その結果，*RP1L1*にR45Wの遺伝子変異が発見され，他2つのオカルト黄斑ジストロフィー家系においても同じ変異が発見された．さらに1家系においてW960R変異が発見された（図4B）[24]．

*RP1L1*は網膜色素変性の原因遺伝子*RP1*に類似する遺伝子としてクローニングされ，多くの患者がスクリーニングされたが遺伝子変異は発見されなかった[25][26]．RP1L1のN末端に対して作製された抗体を用いて免疫染色を行った結果，視細胞の微小管に特異的な染色が観察された（図4C）．この結果はマウスで行われた同様な染色と類似する結果である[27]．視細胞の微小管は高度に分化しており，細胞体と外節の間の輸送機能を担うと同時に視細胞を光軸に沿って細胞の傾きを修正する機能がある[28]．R45WおよびW960Rの遺伝子変異によってこの機能が阻害されると，中心窩の錐体細胞は光軸に対して斜め方向に傾き，感光性は著しく低下する可能性がある．また，錐体細胞はエネルギー消費量が桿体細胞に比べて大きいことから，変異によって微小管の機能が阻害され，細胞輸送が最も盛んな中心窩において，錐体細胞が機能できない状態になっている可能性もある．今後の基礎研究の結果が期待される．

おわりに

黄斑変性のなかから多因子疾患の加齢黄斑変性とメンデル遺伝のオカルト黄斑ジストロフィーを対比しながらご紹介した．相関解析によって得られた感受性遺伝子は環境因子や習慣因子などの影響を受けるために，遺伝子のみの研究では答えが得られない可能性がある．われわれは喫煙，肥満，青色光などのストレスによる影響をこれらのトランスジェニック・ノックアウトマウスを使って検証している．またオカルト黄斑ジストロフィーにおけるRP1L1変異との整合性について，中心窩と周辺部の錐体細胞の構造や光軸に対する傾きの補正について，さらにエネルギー消費量の比較について検討している．加齢黄斑変性とオカルト黄斑ジストロフィーは全く発症機序の異なる疾患であるが，黄斑部の特殊な凹型構造に由来することについては共通している．進化によって，より集光性と感度が高められた結果，逆にストレスに対して脆弱になり，多くの黄斑疾患を伴うようになったと考えられる．黄斑は視覚のなかでも最も重要な部位であり，今後の研究の進展が期待されている．

文献

1) Hoang, Q. V. et al.：Vis. Neurosci., 19：395-407, 2002
2) Klein, R. J. et al.：Science, 308：385-389, 2005
3) Hageman, G. S. et al.：Proc. Natl. Acad. Sci. USA, 102：7227-7232, 2005
4) Okamoto, H. et al.：Mol. Vis., 12：156-158, 2006
5) Gotoh, N. et al.：Hum. Genet., 120：139-143, 2006
6) Pickering, M. C. et al.：Proc. Natl. Acad. Sci. USA, 103：9649-9654, 2006
7) Dewan, A. et al.：Science, 314：989-992, 2006
8) Yoshida, T. et al.：Mol. Vis., 13：545-548, 2007
9) Goto, A. et al.：J. Ocul. Biol. Dis. Infor., 2：164-175, 2009
10) Hollyfield, J. G. et al.：Nature Med., 14：194-198, 2008
11) Yoshida, T. et al.：J. Clin. Invest., 115：2793-2800, 2005
12) Vannas, M. et al.：Eye Ear Nose Throat. Mon.,：50：189-194, 1971
13) Miller, D. M. et al.：Am. J. Ophthal., 138：323-328, 2004
14) Ambati, J. et al.：Nature Med., 9：1390-1397, 2003
15) Nozaki, M. et al.：Proc. Natl. Acad. Sci. USA, 103：2328-2333, 2006
16) Takeda, A. et al.：Nature, 460：225-230, 2009
17) Suzuki, M. T. et al.：Primates, 44：291-294, 2003
18) Umeda, S. et al.：Invest. Ophthalmol. Vis. Sci., 46：683-691, 2005
19) Umeda, S. et al.：FASEB J., 46：1683-1685, 2005